

The X-ray Evaluation of Axially Symmetric Distributions of Fibres in Preferred Orientations

BY E. J. W. WHITTAKER

Ferodo Ltd., Chapel-en-le-Frith, Stockport, England

(Received 16 July 1962)

The intensity distribution in a reflection from a distribution of fibres which is arranged symmetrically about an axis is analyzed in terms of the population density of fibre directions, and a convenient numerical method is developed for the inversion of such an intensity distribution into the corresponding population-density distribution. It is pointed out that the coaxial camera of Hawes has the most advantageous geometry for preferred-orientation studies of this type.

1. Introduction

A crystalline material with a perfectly oriented fibre texture is considered to contain crystallites rotated into all possible azimuths about the fibre axis. Its representation in reciprocal space therefore consists of circles lying on the layer planes perpendicular to the fibre axis. If the fibre orientation is imperfect there will be a distribution of the directions of the fibre axes, each of which will be accompanied in reciprocal space by such an array of circles. The intensity distribution in any given reflection from such a distribution of fibres will therefore depend on the density distribution of the intersections with the sphere of reflection of the corresponding member of these arrays of circles.

2. Diffraction from a fibre of arbitrary direction

Let the mean fibre axis be along OZ , perpendicular to the X-ray beam along OY , and, together with these directions, let OX define a right-handed set of axes. Consider a fibre axis in the direction OQ (Fig. 1) such that $Z\hat{O}Q = \alpha$ and $X\hat{O}R = \beta$, where R is the projection

of Q on the plane XOY . Consider a circle in reciprocal space, of radius ξ , lying on a plane perpendicular to OQ , and distant ζ from O . Let this circle cut the sphere of reflection (centred at $C(0, -1, 0)$ and of unit radius) at P . Let a plane through P parallel to XOZ cut the y -axis at B and the circle of intersection of the sphere with XOY at N . Let $P\hat{B}N = \varphi$.

From the usual considerations of the geometry of reflection

$$\cos Q\hat{O}P = \zeta / (2 \sin \theta)$$

and the direction cosines of OP and OQ are

$$(\cos \theta \cos \varphi, -\sin \theta, \cos \theta \sin \varphi)$$

and

$$(\sin \alpha \cos \beta, \sin \alpha \sin \beta, \cos \alpha).$$

Hence

$$\begin{aligned} \cos \theta \cos \varphi \sin \alpha \cos \beta - \sin \theta \sin \alpha \sin \beta \\ + \cos \theta \sin \varphi \cos \alpha = \zeta / (2 \sin \theta) = \cos \theta \sin \varphi_0 \end{aligned} \quad (1)$$

where $\varphi = \varphi_0$ when $\alpha = 0$.

Introducing the substitution

$$\tan \gamma = \tan \alpha \cos \beta$$

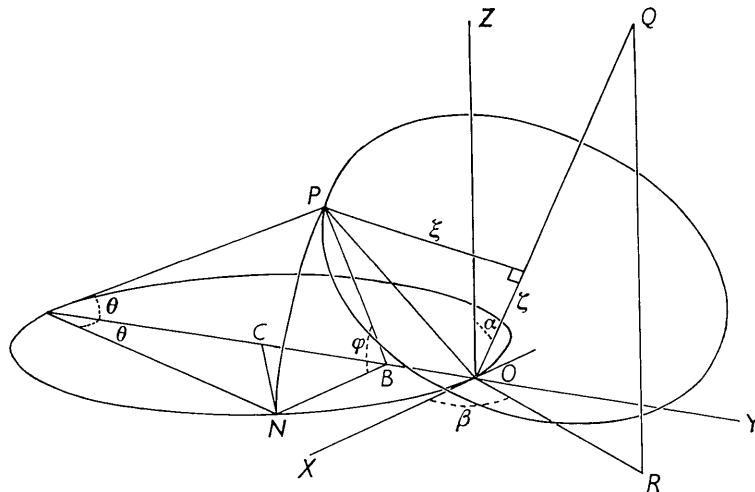


Fig. 1. OZ is the mean fibre axis. OQ is a fibre axis oriented in a direction defined by (α, β) . A circle in reciprocal space centred on OQ , and perpendicular to it, cuts the sphere of reflection at P .

and rearranging, we can show that

$$\sin(\varphi + \gamma) = \sin \gamma \tan \theta \tan \beta + (\sin \varphi_0 \cos \gamma / \cos \alpha). \quad (2)$$

When α is small

$$\sin \gamma \approx \gamma \approx \alpha \cos \beta.$$

Hence

$$\sin(\varphi + \alpha \cos \beta) \approx \alpha \sin \beta \tan \theta + \sin \varphi_0$$

and provided that $(\varphi + \alpha \cos \beta)$ is small

$$\begin{aligned} \varphi - \varphi_0 &\approx \alpha (\sin \beta \tan \theta - \cos \beta) \\ &= (\alpha / \cos \theta) \sin(\beta + \theta - \frac{1}{2}\pi). \quad (3) \end{aligned}$$

The range of validity of the approximations will be examined in § 6 in the light of the use that is made of this formula. In applying the formula to the formation of any particular reflection, it may be simplified by changing the origin of φ and β so that

$$\varphi = \alpha \sin \beta / \cos \theta. \quad (4)$$

3. The effect of a distribution of fibre directions

Let the population density of fibre directions $\rho(\alpha)$ per unit solid angle be axially symmetrical and therefore a function of α only. Then the number in the range

$$\alpha \text{ to } \alpha + d\alpha, \beta \text{ to } \beta + d\beta = \rho(\alpha) \sin \alpha d\alpha d\beta.$$

This will be the number diffracting some particular reflection in the directions φ to $\varphi + d\varphi$ where φ is given by (4), and

$$d\varphi/d\beta = \alpha \cos \beta / \cos \theta.$$

Hence the intensity diffracted in the directions φ to $\varphi + d\varphi$ will be proportional to

$$\begin{aligned} \rho(\alpha) (\sin \alpha \cos \theta / \alpha \cos \beta) d\alpha d\varphi \\ = \rho(\alpha) \sin \alpha \cos \theta (\alpha^2 - \varphi^2 \cos^2 \theta)^{-\frac{1}{2}} d\alpha d\varphi \\ \approx \alpha \rho(\alpha) \cos \theta (\alpha^2 - \varphi^2 \cos^2 \theta)^{-\frac{1}{2}} d\alpha d\varphi. \quad (5) \end{aligned}$$

If $\rho(\alpha)$ were given as an explicit function of α one could therefore integrate the right hand side of (5) to give the total intensity $I(\varphi)$ as a function of φ . The expression is not well adapted, however, for the evaluation of $\rho(\alpha)$ from a measured intensity distribution $I(\varphi)$. A convenient approach is to consider the effect if $\rho(\alpha)$ is constant over a limited range *i.e.*

$$\begin{aligned} \rho(\alpha) &= k \text{ if } 0 \leq \alpha \leq \alpha_1 \\ \rho(\alpha) &= 0 \text{ if } \alpha > \alpha_1 \end{aligned}$$

Hence

$$\begin{aligned} I(\varphi) &= k \cos \theta \int_{\varphi \cos \theta}^{\alpha_1} (\alpha^2 - \varphi^2 \cos^2 \theta)^{-\frac{1}{2}} d\alpha \\ &= k \cos^2 \theta (\alpha_1^2 \sec^2 \theta - \varphi^2)^{\frac{1}{2}}. \quad (6) \end{aligned}$$

In this integration it is permissible to use $\varphi \cos \theta$ as the lower limit of integration, rather than zero, because any fibre for which $\alpha < \varphi \cos \theta$ does not contribute to the intensity in the direction φ .

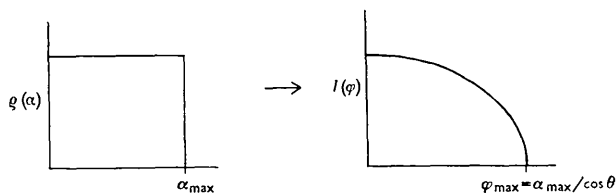


Fig. 2. Correspondence between a uniform population density of fibre directions $\rho(\alpha)$, and the resulting distribution of X-ray intensity $I(\varphi)$.

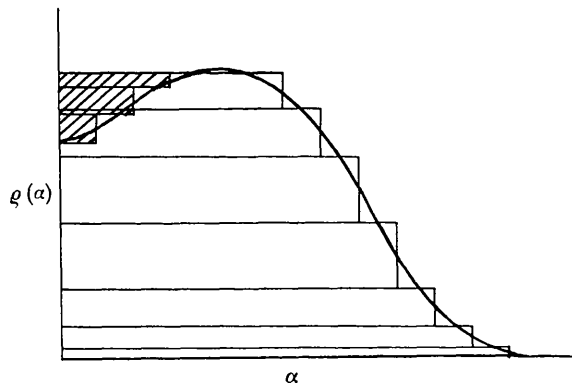


Fig. 3. Division of an arbitrary function $\rho(\alpha)$ into components of uniform population density. Negative components are shaded.

Thus the intensity profile is a semi-ellipse of height $k\alpha_1 \cos \theta$ centred at $\varphi=0$, and with a horizontal semi-axis of $\alpha_1 \sec \theta$. Fig. 2 shows the relationship between a uniform density distribution of fibre directions and the resulting intensity profile according to (6), for positive values of φ . It follows that if any arbitrary intensity distribution such as that in Fig. 3 were divided into horizontal rectangular areas, positive or negative, each of these would give rise to an elliptical intensity profile, positive or negative, and these could be summed to give the total intensity profile. Conversely if an arbitrary given intensity profile could be analyzed as a sum of (positive and negative) elliptical elements then the corresponding density distribution of directions could easily be evaluated.

4. Inversion of the intensity distribution

It must be assumed that the intensity is effectively zero for $\varphi > \varphi_n$. The procedure is then as follows:

- (1) Take the $n+1$ values of $I_0 \dots I_n$ at equal intervals $\varphi_0 \dots \varphi_n$. From these derive the corresponding n values of $I_0 - I_1, \dots, I_{n-1} - I_n = \Delta I_1 \dots \Delta I_n$.
- (2) Prepare a master table of values

$$\begin{aligned} \Delta y_{1,0} \dots \Delta y_{q,0} \dots \Delta y_{n,0} \\ \dots \\ \Delta y_{1,r} \dots \Delta y_{q,r} \dots \Delta y_{n-r,r} \\ \dots \\ \Delta y_{1,n-1} \end{aligned}$$

where

$$y_{q,r} = ((n-r)^2 - q^2)^{\frac{1}{2}}$$

and

$$\Delta y_{q,r} = y_{q-1,r} - y_{q,r}$$

(3) The amplitude at $\varphi=0$ of the elliptical component of the intensity which extends to φ_n is then given by

$$\Delta I_{n,y_{0,0}} / \Delta y_{n,0} = A_n \cdot y_{0,0}$$

A_n is then the height of the elementary rectangle of $\varrho(\alpha)$ which extends to $\alpha = \varphi_n \cos \theta$.

This will make a contribution $A_n \cdot \Delta y_{q,0}$ to each of the other values of ΔI_q . The elliptical component which extends to φ_{n-1} can therefore be determined by taking

$$A_{n-1} = (\Delta I_{n-1} - A_n \cdot \Delta y_{n-1,0}) / \Delta y_{n-1,1} \quad (7)$$

and this is the height of the elementary rectangle of $\varrho(\alpha)$ which extends to $\alpha = \varphi_{n-1} \cos \theta$. The process may be continued step by step, and in general

$$A_{n-q} = [\Delta I_{n-q} - \sum_{p=0}^{q-1} A_{n-p} \Delta y_{n-q,p}] / \Delta y_{n-q,q} \quad (8)$$

A convenient numerical procedure is as follows:

- (i) Find A_n as above.
- (ii) Multiply all the values of $\Delta y_{q,0}$ (the first line of the Δy table) by A_n , and enter the products in the first line of a second similar table of $A_{n-r} y_{q,r}$.
- (iii) Find A_{n-1} from equation (7).
- (iv) Multiply all the values of $\Delta y_{q,1}$ by A_{n-1} and enter the products in the second line of the table of $A_{n-r} y_{q,r}$.
- (v) Sum of the values in the $(n-1)$ th column of this table and hence calculate A_{n-2} from equation (8).
- (vi) Continue to calculate successive lines of the table. Each line leads to the completion of a further column whose sum can be used in equation (8) to give the next value of A_{n-q} .

4. When all the values of A_{n-q} have been calculated the function $\varrho(\alpha)$ can be calculated, in stepped form, at $n+1$ equidistant points from $\alpha=0$ to $\varphi_n \cos \theta$ from the formula

$$\varrho(\alpha_{n-q}) = \sum_0^q A_{n-q} \quad (9)$$

5. Check of the numerical method

The arbitrary density distribution shown in Fig. 4(a) was divided into horizontal rectangles terminating at 17 equally spaced values of the abscissa. The corresponding intensity distribution (Fig. 4(b)) was then calculated by summation of the effects of each of these rectangular density distributions as given by equation (6). This intensity distribution was then inverted back to a density distribution using $n=10$ and $n=7$, with the results shown in Fig. 4(c). The numbers of intervals were chosen to be prime with

respect to those used in the synthesis of Fig. 4(b) in order to provide a reasonable test of the method. Clearly the width of the intervals must not be less than that of any maximum or minimum which it is desired to reveal, but within this limitation the method gives a satisfactory reproduction of the form of the original density distribution. A value of n in

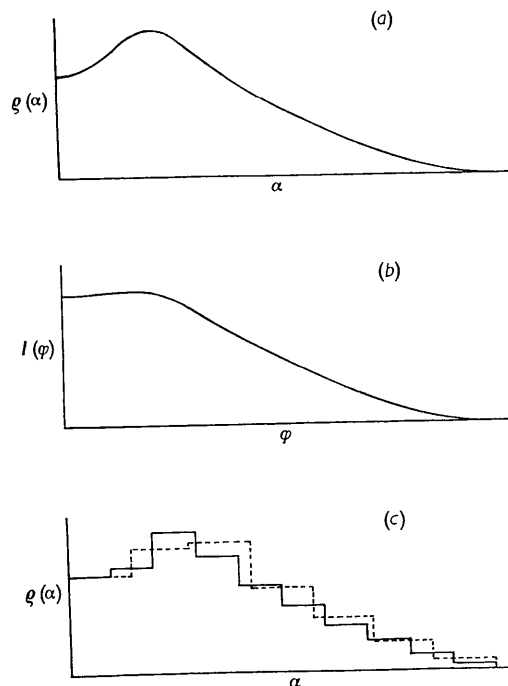


Fig. 4. (a) Arbitrary population density distribution. (b) Corresponding intensity distribution calculated from (a) using 17 intervals. (c) Inversion of (b) to population density in stepped form using 10 intervals (full line) and 7 intervals (broken line).

the range from 10 to 20 is likely to be suitable for most purposes. The amount of computation involved increases as n^2 . In Fig. 4(c) the heights of the curves have been scaled to agree with that of Fig. 4(a). The absolute numerical values obtained by the method depend not only on the value of n used but also on the actual form of the $\varrho(\alpha)$ curve, and cannot be simply predicted.

6. The range of validity of the approximations and consideration of errors

The most extreme assumption made in the small-angle approximations in § 2 is that $(\varphi + \alpha \cos \beta)$ is small. But

$$\begin{aligned} |\varphi + \alpha \cos \beta| &\leq |\varphi| + |\alpha \cos \beta| \\ &\leq |\varphi| + |\alpha| \\ &\leq 2|\varphi| \end{aligned}$$

The actual error varies with β , but is always less than 5% for $|\varphi| < 15^\circ$ and less than 2% for $|\varphi| < 10^\circ$.

Since it is necessary that 2φ be small it follows

that the method is most satisfactory for reflections on zero layer lines. For a reflection on a non-zero layer line

$$\tan \varphi_0 = \zeta / [\sin \gamma (1 - \zeta^2)^{\frac{1}{2}}]$$

so that the minimum value of φ_0 is obtained when the azimuth of the reflection, γ , is 90° . Even here, however, the approximations will be valid only for a very restricted range of α , unless ζ is very small, in view of the restrictions on φ . Furthermore, since

$$(\varphi - \varphi_0)_{\max} = \alpha_{\max} / \cos \theta$$

it is desirable that $\cos \theta$ should be as large as possible. For reflections on non-zero layer lines it is therefore desirable to keep γ as much smaller than 90° as is compatible with keeping φ_0 small. For reflexions on the zero layer line it is always better to use fairly low-angle reflections, though the effect does not become very important for $\theta < 30^\circ$.

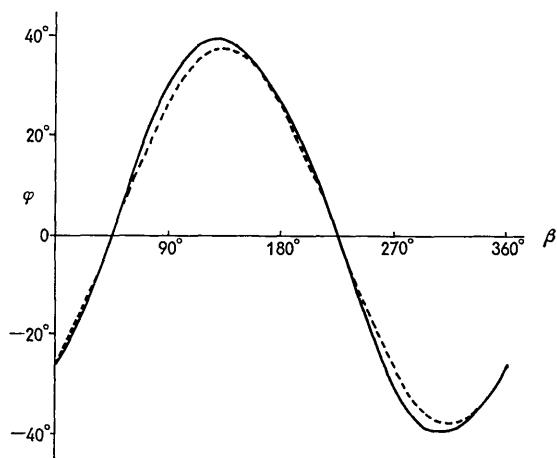


Fig. 5. The angle φ as a function of β for $\theta = 45^\circ$, $\alpha = 26\frac{1}{2}^\circ$. The full line shows the true value from equation (2) and the broken line the approximation of equation (3).

Fig. 5, shows the way in which the approximate value of φ tends to depart from the true value. To make the separation of the curves clear they have been calculated for $\theta = 45^\circ$ and $\alpha = 26\frac{1}{2}^\circ$, *i.e.* substantially larger than those recommended.

Since a zero-layer-line reflection from a material with fibrous orientation will usually have its greatest intensity near $\varphi = 0$ and will fall away to low intensities at large φ , it follows that the regions in which the approximations involve the largest errors will be those of the least significance. Even errors in excess of 5% may be quite acceptable in these regions, so that the method may be applied even when $\varphi_{\max} > 15^\circ$.

In view of the iterative nature of the numerical procedure discussed in § 4 it is desirable to ascertain whether it may introduce cumulative errors. If we denote the errors in A_{n-q} , ΔI_{n-q} and $\Delta y_{n-q,p}$ by δA_{n-q} , δI_{n-q} and $\delta y_{n-q,p}$ respectively, then differentiation of equation (8) leads to

$$\delta A_{n-q} = \frac{\delta I_{n-q}}{\Delta y_{n-p,q}} - \sum_{p=0}^{q-1} \delta A_{n-p} \frac{\Delta y_{n-q,p}}{\Delta y_{n-q,q}} - \sum_{p=0}^q A_{n-p} \frac{\delta y_{n-q,p}}{\Delta y_{n-q,q}}, \quad (10)$$

The third term involves only the rounding off errors in the table of $\Delta y_{n-q,p}$, and these, though cumulative, may be made as small as we please. With n in the range 10–20 the effect of this term will be negligible if the table of Δy is prepared to three decimal places. The second term then depends only on the errors arising from δI_{n-p} and (10) may be expanded into the form

$$\delta A_{n-q} = \frac{\delta I_{n-q}}{\Delta y_{n-q,q}} - \sum_{p=0}^{q-1} a_{n-p} \delta I_{n-p}$$

where the coefficients a_{n-p} are all positive and decrease monotonically with p . But since the values ΔI_{n-p} are successive differences their errors are not independent and

$$\sum_{p=0}^{q-1} \delta I_{n-p} \sim \delta I_{n-q+1}.$$

Hence

$$\delta A_{n-q} \sim \frac{\delta I_{n-q}}{\Delta y_{n-q,q}} - \frac{\delta I_{n-q+1} \Delta y_{n-q,q-1}}{\Delta y_{n-q+1,q-1} \Delta y_{n-q,q}}.$$

Therefore the errors δI do not lead to cumulative errors in A_{n-q} . It follows similarly that the errors are again non-cumulative when $\varrho(\alpha_{n-q})$ is evaluated by the summation of the terms A_{n-q} in equation (9).

7. Practical considerations

If the diffraction pattern is recorded in a cylindrical camera of conventional design the intensity distribution must be measured along a Debye curve of constant θ , and the path length along this curve transformed into terms of φ . Neither of these processes is very convenient, and furthermore the intensity distribution along the line will be modified by a varying obliquity effect. Recording on a flat film perpendicular to the beam leads to some improvement since the lines of constant θ are then circular, but the most convenient method of recording for orientation studies is a coaxial camera, such as that described for a different purpose by Hawes (1959), in which the film lies on a cylinder coaxial with the beam. Lines of constant θ are then straight lines, and φ is directly proportional to distance along these lines.

I wish to thank the Directors of Ferodo Ltd., for permission to publish this paper.

Reference

HAWES, L. L. (1959). *Acta Cryst.* **12**, 443.